

Simulation study on spatial distribution of organic carbon in erosion gullies in Heilongjiang Province based on geostatistical methods

Hongfeng Wang^{1,2}, Xingchen Yu^{3,*}, Yanda Lu^{1,2}, Jiuyi Wang^{1,2} and Ye Luo^{1,2}

¹ Harbin Center for Integrated Natural Resources Survey, China Geological Survey, Harbin, Heilongjiang, 150086, China

² Observation and Research Station of Earth Critical Zone in Black Soil, Ministry of Natural Resources, Harbin, Heilongjiang, 150086, China

³ Yantai Center of Coastal Zone Geological Survey, China Geological Survey, Yantai, Shandong, 264000, China

Corresponding authors: (e-mail: yxc401918225@163.com).

Abstract Heilongjiang Province is an important agricultural production base in China, and its soil organic carbon stock occupies an important position in the country. In recent years, the spatial distribution of soil organic carbon has gradually received wide attention with the environmental changes and the transformation of agricultural production methods. By studying the spatial distribution characteristics of soil organic carbon in erosion gully area, it can provide scientific basis for regional soil protection and carbon sink management. This paper discusses the spatial distribution characteristics of soil organic carbon in erosion gully area and its simulation method based on the geostatistical method in Heilongjiang Province. The study collected soil samples from different points in the erosion gully area, and used geostatistical methods to spatially analyze and simulate the soil organic carbon data. The study firstly determined the best semi-variance function model by calculating the spatial correlation of the sample points, and then predicted the spatial distribution of soil organic carbon by using the Kriging interpolation method. The results show that the spatial distribution of soil organic carbon in the erosion gully area has obvious regional differences and is jointly influenced by topography, vegetation cover and land use type. Through the simulated spatial distribution maps, areas with higher organic carbon storage and plots with higher carbon sink capacity can be clearly seen. This study provides a scientific basis for further soil protection measures, carbon sink management and sustainable agricultural development.

Index Terms spatial distribution simulation, organic carbon distribution, erosion gully, geographically weighted regression model, kriging interpolation

I. Introduction

Heilongjiang Province is the second province in China with grain output exceeding 100 billion kilograms, ranking first in the country in terms of grain commodities and transfers, with abundant arable land resources and high potential for increasing grain production, yet erosion gully disasters are intensifying in this grain-producing province [1]-[3]. Erosion gullies are trough-shaped depressions formed by the scouring of soil after natural rainfall convergence, small erosion gullies are like cracks in the land, and large erosion gullies, are gullies up to dozens of meters in width and stretching over several kilometers [4]-[6]. The area of affected cropland around an erosion gully exceeds several times its own footprint, and it cuts intact cropland into pieces, reduces the area of cropland, makes it impossible for large-scale agricultural machines to plow, and decreases land utilization [7]-[9]. Moreover, with gradual development and deterioration, erosion gullies devour good downstream fields and bring sediment to the cultivated land, resulting in a decrease in food production and threatening food security [10], [11]. Therefore, erosion gully is considered as one of the most obvious, direct and serious hazards in soil erosion with the most obvious impacts, and one of the important causes of the serious destruction of black soil in Heilongjiang [12], [13].

And the spatial distribution of organic carbon in erosion gullies refers to the storage and change law of carbon elements in different geographic areas, soil types and depth levels [14], [15]. Soil organic carbon is a carbon-containing substance formed by the transformation of plant and animal residues and microbial metabolites in specific environmental conditions, which is stored in the soil to form a "carbon pool" [16], [17]. The spatial distribution includes both horizontal dimension (different latitude, altitude, geomorphic unit differences) and vertical dimension (different soil depth differences), and its influencing factors can be summarized into two categories: natural elements and human activities [18], [19]. Understanding the spatial distribution of organic carbon in erosion gullies in Heilongjiang Province is of practical significance for agricultural production, ecological protection, and climate change response [20].

This paper focuses on the spatial distribution of organic carbon in erosion gullies in Heilongjiang Province, and studies the specific effects of natural climate and other factors on soil organic carbon content. The spatial information of erosion gullies is extracted by remote sensing technology and relevant basic data are generated. The determination of soil organic carbon and its components was completed step by step according to the steps of making soil samples, measuring carbon components and calculating density. The basic physical and chemical properties of the soil were further determined by methods such as volumetric weighing and water immersion. Kriging interpolation based on spatial autocorrelation was utilized to predict the soil organic carbon content at different locations. Afterwards, a random forest algorithm was used to assess the influence of topography and other factors on the distribution of soil organic carbon in erosion gullies, and a geographically weighted regression model was constructed.

II. Analysis of research objects and research methods

II. A. Analysis of information related to the study area

II. A. 1) Overview of the study area

County A is located in the western part of Heilongjiang Province, elevation of 60-336m, is located in the small xinganling remnants and the Songnen Plain hilly area, the terrain tilted from northeast to southwest, from the east of the small xinganling mountains before the high plains, the transition to the southwest for the low plains, sandwiched between the uyueer river and the tongkeng river, with jurisdiction over 8 towns and 12 townships. County A has a total land area of 3,650km², of which 2,770km² is arable land, and crops are mainly cultivated in dry fields, which is a typical agricultural county and a famous ecological county. The study area belongs to the mid-temperate continental monsoon climate, with severe cold in winter, short and rainy summer, large temperature difference between the four seasons, average annual temperature of 1.5°C, and average annual precipitation of 450mm; the characteristics of the black soil area, such as poorer soil erosion resistance, concentrated rainfall, undulating terrain, and long-term high-intensity agricultural production, have caused serious soil and water erosion.

II. A. 2) Data sources

The 2020 SPOT5 satellite image and the 2024 Gaofen-1 remote sensing image of County A, with spatial resolutions of 2.8 and 2.5 m, respectively, were extracted at the time corresponding to April and November, and the images in this period had few clouds and good quality, which made it easy to distinguish the morphological features of erosion gullies. The topographic data were obtained from the DEM data of the geospatial data cloud website with a resolution of 13 m. The administrative boundaries were obtained from the database of the Third National Land Survey of County A, and the map precision was 1:10,000.

II. A. 3) Erosion gully spatial information extraction methods

In order to accurately extract the spatial information of erosion gullies in the study area in 2020 and 2024, the remote sensing images were geometrically corrected and projected to form orthophotos with a projected coordinate system of 2500 national geodetic coordinate system, and the markers for interpreting the spatial information of erosion gullies were created based on the spectral characteristics of the images in the study area as well as the texture and color characteristics of the erosion gullies. Taking the 2020 and 2024 images as the basic data source, we extracted the erosion gully valley lines, range surfaces and river data of the two years through visual interpretation, in which the erosion gully valley lines were based on the length of the center line, and the range surfaces were based on the range of the outer edge line of the erosion gully, and we combined the comprehensive work of field research and field validation to further validate and modify the number and morphology of the erosion gully and finally obtain the 2020 and 2024 erosion gully data of A county. The spatial distribution vector data of erosion gully in 2020 and 2024 were finally obtained. On this basis, ArcGIS surface analysis tool was used to generate slope and slope direction raster data from DEM data, and Euclidean distance tool was used to generate distance raster data from river data.

II. B. Determination and calculation of soil organic carbon (SOC) and its fractions

II. B. 1) Soil organic carbon grouping

The SOC was divided into two groups, particulate organic carbon (POC) and mineral bound organic carbon (MAOC), as follows: 25 g of air-dried soil was well dispersed by shaking with 150 ml of 10% concentration of sodium hexametaphosphate (NaHMP) for 24 hours. The dispersed soil was then washed through a 55 μm sieve on an analytical sieving apparatus. During this process, the soil on the sieve was washed with deionized water until the sieve ran clear. The fraction remaining on the sieve was considered POC, while the finer fraction passing through the sieve was considered MAOC.

II. B. 2) Measurement of soil organic carbon

Determination of organic carbon and its components is mainly divided into two steps: 1) acidification of the soil: first configure 2 mol / L hydrochloric acid solution, prepare the centrifuge tubes and numbering, centrifuge tubes were put into 2.5g of air-dried soil and 15 ml of hydrochloric acid solution so that it is fully acidified (shaking until it does not produce air bubbles), static overnight into the centrifuge to 5000r/min centrifugation for 5min, will be poured off the top. The supernatant was poured off - water was added - shaken well - centrifugation process was repeated three times and then put into the oven for drying, after drying, ground and bagged for testing; 2) Determination of soil organic carbon and total nitrogen: The soil sample after grinding is wrapped with tinfoil for sample treatment, the sample weight is about 45mg, numbered for measurement, and then the soil sample is put into the elemental analyzer for measurement, because the acidification is treated with the inorganic carbon component in the soil, so the soil organic carbon and total nitrogen content can be calculated according to the data in the elemental analyzer.

II. B. 3) Calculation of soil organic carbon density

Soil organic carbon density refers to the soil organic carbon storage under a certain thickness per unit area, which is an important indicator reflecting the nature of the soil, this study focuses on the organic carbon density of the surface soil (0-25cm), which is calculated by the following formula:

$$SOCD = SOC(I) \times \gamma(I) \times h \times 10^{-2} \quad (1)$$

where, $SOCD$ represents the soil organic carbon density (kg / m^2)

$SOC(I)$ represents the soil organic carbon content of the top soil (g / kg)

$\gamma(I)$ represents the soil bulk weight of the top soil (g / cm^3).

h represents the soil thickness of the soil layer (cm)

II. B. 4) Calculation of soil particulate organic carbon and mineral-bound organic carbon content

The formulas for calculating POC and MAOC content are shown below:

$$POC \text{ content} (g / kg) = POC \text{ concentration} (g / kg) \times \frac{POC \text{ mass} (g)}{\text{soil mass} (g)} \times 100 \quad (2)$$

The principle of calculation of MAOC content is similar, that is, just replace the above POC with MAOC.

II. C. Determination of basic physical and chemical properties of soil

The basic physical and chemical properties of the soil need to be determined in the laboratory, the main determinations were water content, bulk density, pH, and conductivity.

II. C. 1) Determination of soil mass moisture content and soil bulk weight

Soil mass moisture content and bulk weight were determined as follows: soil samples taken with a ring cutter were placed in an aluminum box of known weight m_0 , the weights of the box and the soil samples were recorded m_1 , the box was subjected to drying process in an oven at 100°C, and the weights of the box and its soil samples were again recorded and recorded as m_2 . The formula is calculated as follows:

$$W (\text{Mass moisture content}) = (m_2 - m_1) / (m_2 - m_0) \times 100 \quad (3)$$

where, m_1 is the weight of the aluminum box and soil sample $m_1(g)$.

m_2 is the weight of dried aluminum box and soil sample (g).

m_0 indicates the weight of the empty aluminum box (g).

W is the water content.

The formula for calculating the soil bulk weight is as follows:

$$BD (\text{Soil capacity}) = (m_2 - m_0) / 100 \quad (4)$$

II. C. 2) Determination of soil pH and conductivity

Soil pH and conductivity were determined as follows: Soil pH was determined by water immersion, mainly by extracting the pH of the soil with distilled water, which represents the active acidity of the soil. The process is as follows: take 6g of soil, according to the water-soil ratio of 6:1 ratio of water added to the centrifuge tube, through

the vortex mixer shaking well, in the determination of the standard buffer needs to be calibrated, calibration is complete, with the soil pH meter for measurement, in order to reduce the error of the measurement of each sample three times, take the average as the pH value of the sample measured. The determination of conductivity is basically the same as that of pH, and the instrument used is a conductivity meter.

II. D. Analysis of research methodology

II. D. 1) Geographically weighted regression models

Geographically weighted regression model is a kind of local regression model, which is developed on the basis of linear model. The geographically weighted regression model is based on different geospatial locations and spatially analyzes the variable factor indicators in the region with the explanatory variable factor indicators to realize the local spatialized expression of the data.

$$Y_i(\lambda_i, \vartheta_i) = \beta_0(\lambda_i, \vartheta_i) + \sum_{i=1}^n \beta_n(\lambda_i, \vartheta_i) \chi_i(\lambda_i, \vartheta_i) + \delta_i \quad (5)$$

where, $Y_i(\lambda_i, \vartheta_i)$ is the predicted value of the dependent variable at sample location i ; and $\beta_0(\lambda_i, \vartheta_i)$ is the value of the intercept size; $\beta_n(\lambda_i, \vartheta_i)$ is the regression coefficient of sample point i at n ; and (λ_i, ϑ_i) is the geographic coordinate of point i in the sample site; $\chi_i(\lambda_i, \vartheta_i)$ is the value of the environmental factor and the physicochemical factor at the i th sample point; δ_i is the simulated residual term at the i th sample point.

The spatial distance weights are calculated considering the bandwidth, and the simulation accuracy of the GWR model is affected by the bandwidth of the model, which is partitioned in this study by correcting the Akaike Information Criterion (AIC), with A_{ICc} as the selection criterion for the bandwidth.

$$A_{ICc} = A_{IC} + \frac{2K(K+1)}{n-K-1} \quad (6)$$

$$A_{IC} = 2K - 2\ln(L)$$

where, n is the number of observations; K is the number of independent parameters of the model; L is the great likelihood function of the model.

II. D. 2) Random Forest Model

Random Forest (RF) is a non-parametric algorithm that can rank the importance of influencing factor variables, quickly identify the main influencing factors among multiple factor variables, and has strong applicability in the classification processing of data. The computational principle of the random forest model is to randomly build a decision tree on an existing data set that needs to be trained, and build each data node on the decision tree, and seek to take out the average value of the data as the result of the decision tree output. In this study, based on the random forest algorithm, the importance of terrain, climate external environmental influences and soil internal physical and chemical properties on soil organic carbon was calculated, and the Bootstrap resampling method was used to construct the regression tree for node splitting multiple times.

II. D. 3) Kriging Interpolation

Three-dimensional geological modeling commonly used analysis means for spatial interpolation analysis, Kriging interpolation method is a commonly used method for the analysis of soil organic carbon content, in the study of the regionalization of erosion gully organic carbon variables in the spatial distribution of structural characteristics of regularity, based on a comprehensive consideration of the spatial variables of the randomness and structural nature of a mathematical geological method. Kriging interpolation maximizes the use of all kinds of information provided by the exploration project, and when using the Kriging interpolation method to estimate the average value, the spatial location relationship between the location to be estimated and the information samples, the spatial location relationship between the information samples and each other, as well as the structural characteristics of the spatial distribution of the regionalized variables, etc., are fully taken into account. The core of the kriging interpolation method lies in assigning appropriate weighting coefficients to the sample data of each organic carbon component, which can give a more realistic and accurate estimation, and the method can avoid systematic errors. The simple kriging formula is shown in equation (7).

$$Z^* = \sum_{i=1}^n X_i W_i \quad (7)$$

where Z^* is the unknown point information to be sought; X_i is the known point data; and W_i is the weight of the point, with all weights summing to 1.0.

III. Simulation experiment on the spatial distribution of organic carbon in erosion gullies

III. A. Overview of erosion gully development and regularity analysis

III. A. 1) Overview of erosion gully development

Table 1 summarizes the statistics of changes in the number, area, and length of erosion gullies within County A from 2020 to 2024. The number of erosion gullies in 2024 increased by 19.33% from 2020, the number of development gullies increased by 5.39%, the number of stabilization gullies increased by 26.39%, and the density of erosion gullies increased by 42.86%, while the area and length of erosion gullies increased by 241.16% and 20.52%. Erosion gullies gradually increase, deepen and become longer. Erosion gullies are better developed in 2024 than in 2020, indicating that erosion in County A is increasing and showing more damage.

Table 1: Variation of erosion gullies from 2020 to 2024

Indicator	Year		Growth quantity	Growth Rate (%)
	2020	2024		
Number of erosion gullies (pieces)	26734	31902	5168	19.33
Number of development ditches (pieces)	20172	21320	1148	5.39
Number of stable ditches (pieces)	18290	23115	4825	26.39
Density of gullies (km·km ⁻²)	0.21	0.30	0.09	42.86
Erosion gully area (km ²)	147.7	503.6	355.9	241.16
Length of erosion gully (km)	12983	15649	2666	20.52

III. A. 2) Cumulative analysis of erosion gully density slope development volume

Slopes of different gradients have a large impact on the development and distribution of erosion gullies, and this section analyzes the impact of specific gradients on erosion gully development. Figure 1 shows the cumulative results of erosion gully density slope development volume. The development of erosion gully densities of different slopes are added up, and the development of 8 major slopes reaches 15.40 gully/km². 4.5-8° slopes have the most intensive development and distribution of erosion gully, reaching 3.69 gully/km², which is because the slope is between smooth and sloping, and is easy to be eroded by rainwater. The least intensive is 30-95°, where rainwater has less force due to the excessive inclination, and therefore the intensity is only 0.52/km².

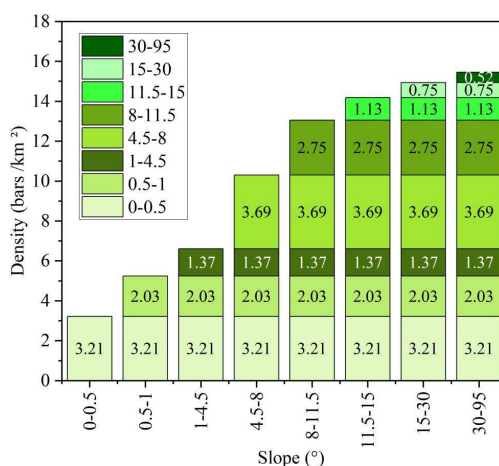


Figure 1: Accumulative chart of gully intensity increment in different slope

III. B. Characteristics of spatial differentiation in the content of soil organic carbon fractions

III. B. 1) Characteristics of the horizontal distribution of MAOCs

Table 2 characterizes the horizontal distribution of MAOC. From the distribution of MAOC levels in different sampling sites, the highest value of MAOC was found in the agricultural field at sampling site G (14.66±1.15g/kg) and the lowest value was found in H (4.11±8.51g/kg); the highest value of MAOC was found in grassy flats at D (25.25±4.64g/kg) and the lowest value was found in C (14.14±4.51g/kg); the highest value of MAOC was found in

C ($25.41 \pm 4.56 \text{g/kg}$) and the lowest value was in E ($14.48 \pm 2.56 \text{g/kg}$) in the mudflat; the highest value of MAOC was found in G ($64.54 \pm 1.61 \text{g/kg}$) and the lowest value was in D ($14.14 \pm 1.46 \text{g/kg}$) in the shallow water area. Significant differences ($P < 0.05$) were observed in MAOC content between sampling sites.

Table 2: Distribution of surface MAOC content at different sampling points

Sampling point	Farmland(g/kg)	Grassland(g/kg)	Mudflat(g/kg)	Shallow water area(g/kg)
A	14.51 ± 1.64	25.24 ± 4.56	24.84 ± 6.15	26.48 ± 2.21
B	14.41 ± 2.66	14.54 ± 8.54	18.84 ± 2.81	14.21 ± 1.16
C	14.25 ± 6.58	14.14 ± 4.51	25.41 ± 4.56	14.15 ± 6.61
D	11.46 ± 8.51	25.25 ± 4.64	21.14 ± 1.66	14.14 ± 1.46
E	14.46 ± 1.84	16.15 ± 1.24	14.48 ± 2.56	16.15 ± 4.26
F	11.66 ± 2.22	21.64 ± 5.11	16.58 ± 1.65	15.54 ± 8.54
G	14.66 ± 1.15	16.65 ± 6.64	16.58 ± 1.65	64.54 ± 1.61
H	4.11 ± 8.51	15.11 ± 1.66	16.58 ± 1.65	28.56 ± 1.61

III. B. 2) Vertical Distribution Characteristics of the MAOC

The vertical distribution characteristics of MAOC in grassy flats and mud carbon are used as an example to analyze the vertical distribution characteristics of MAOC in erosion gullies in County A. Figure 2 shows the vertical distribution of MAOC in erosion gullies in County A. By analyzing the MAOC data, it was found that the distribution range of MAOC content of grassy beach was between $9.63\text{--}29.89 \text{g/kg}$, and the MAOC content of each soil layer from shallow to deep was 26.89g/kg , 14.91g/kg , 12.80g/kg , 10.40g/kg , 10.14g/kg , 9.74g/kg . The distribution of mudflats ranged from 11.92 to 29.97g/kg , and the MAOC contents of each soil layer from shallow to deep were 27.79g/kg , 17.77g/kg , 16.21g/kg , 15.04g/kg , 13.37g/kg , and 12.24g/kg , respectively. Observation of the changes in MAOC contents of grassflats revealed that in the vertical direction The MAOC content of the grassy bank showed an obvious decreasing trend with the deepening of the soil depth, and the MAOC was obviously concentrated in the top soil layer (0-25cm), and the MAOC content of the 0-15cm soil layer was significantly higher than that of the other layers. The MAOC content in the 15-25 cm soil layer was significantly different from that in other soil layers, and the MAOC content in the soil layers after 25 cm was comparable, and the trend of change was not obvious enough; among the mudflats, the MAOC content in the vertical direction also showed a trend of gradual decrease with the deepening of the soil layer, and the MAOC was concentrated in the top soil layer (0-25 cm), and the MAOC content in the 0-15 cm soil layer showed a clear decreasing trend, and MAOC was obviously concentrated in the top soil layer (0-25 cm). 15cm soil layer MAOC content was significantly higher than the other layers, the MAOC content in the 15-25cm soil layer was significantly different from the other layers, and the MAOC content was comparable among the soil layers after 25cm, with no significant difference and a slow trend of change.

Overall, the MAOC content of erosion gullies in County A all decreased continuously with the depth of soil layer, and all of them started to change at a faster rate and then gradually changed at a gentle pace. Further observation revealed that the average MAOC content of mudflats was obviously larger than that of grassflats, and except for the top 0-15cm soil layer, the average MAOC content of mudflats was larger than that of grassflats in the 15-105cm soil layer, indicating that mudflats were more favorable for MAOC storage than grassflats, probably because mudflats themselves had larger water content and were less hazardous to erosion than grassflats.

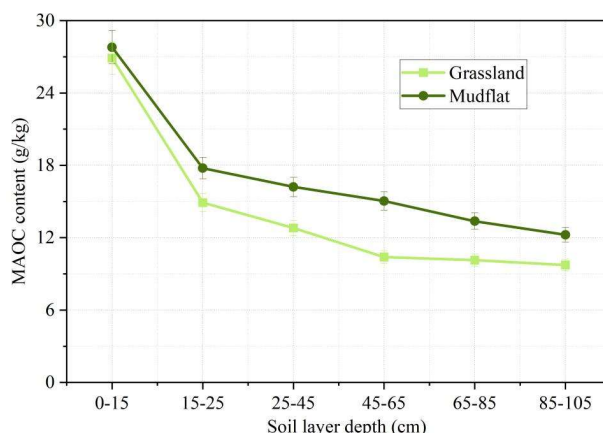


Figure 2: Vertical distribution of MAOC content in erosion gullies of County A

III. B. 3) Vertical Distribution Characteristics of POCs

Figure 3 shows the vertical distribution of POC in erosion gullies in County A. Vertically, the distribution of POC content in the grassy bank ranged from 1.60 to 14.78 g/kg, and the POC content of each soil layer from shallow to deep was 14.78 g/kg, 3.81 g/kg, 2.46 g/kg, 2.17 g/kg, 2.17 g/kg, and 1.60 g/kg, respectively. The distribution of mud bank ranged from 2.43 to 18.13 g/kg. The POC content of each soil layer from shallow to deep was 18.13g/kg, 16.66g/kg, 5.35g/kg, 4.77g/kg, 3.66g/kg, and 2.43g/kg, respectively. The POC content of the grassy bank erosion gully in County A showed a significant decreasing trend with the deepening of the soil layer depth, unlike the MAOC, and the grassy bank POC was obviously concentrated in the surface layer of 0 -15cm soil, and the POC content in the 0-15cm soil layer was significantly higher than that in the deeper soil layer. The POC content between the deeper soils below the 0-15 cm topsoil was comparable, not significantly different, and the trend was not significant. Similarly, the POC of mudflats also showed a trend of gradual decrease with deepening of soil depth in the vertical direction, which was consistent with the MAOC, and the POC of mudflats was obviously concentrated in the top soil layer of 0-25 cm, and was significantly higher than that of all deeper soils below 25 cm. the POC values were lower and the difference was not significant among the soil layers below 25 cm, and the change tended to be flat.

In general, it seems that the POC content of erosion gullies in both grass and mud flats in County A showed a tendency to decrease with soil depth, i.e., the change was large at the beginning and then slowed down. However, the change trends of grass and mudflats were slightly different, with the grass flats showing a large change in magnitude, which is a sudden decrease, while the change of POC in mudflats was slightly slower, which is a decreasing trend. Similar to MAOC, mudflats are more favorable for the storage of particulate organic carbon than grassflats, and the particulate organic carbon in mudflats is more stable and not easy to decompose.

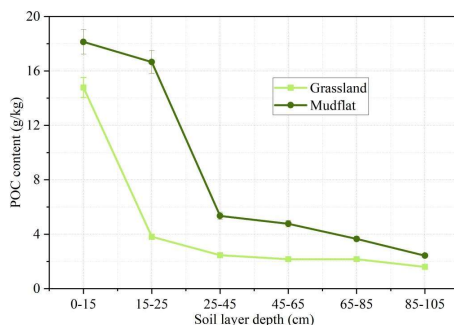


Figure 3: Vertical distribution of POC content in erosion gullies of County A

III. C. Regression analysis of erosion modulus and soil organic carbon content

The content of different components of organic carbon in the 0-25 cm soil layer of different land types of erosion gullies at each sampling site in County A was regression analyzed with the soil erosion modulus, respectively. The results of the regression analysis are shown in Fig. 4. The coefficients of determination of MAOC, POC, CPOC, and FPOC were 0.07603, 0.12069, 0.49331, and 0.53291, respectively. In the regression analysis of the content of different components of organic carbon and the erosion number, the points of erosion modulus were not very discrete, so that the influence of hydraulic erosion on each organic carbon component was more obvious. It is generally believed that fine and light organic carbon is easy to be enriched in fine-grained sediment and subsequently undergoes preferential migration and deposition, which is greatly influenced by hydraulic factors and is prone to form erosion gullies under the addition of different slopes.

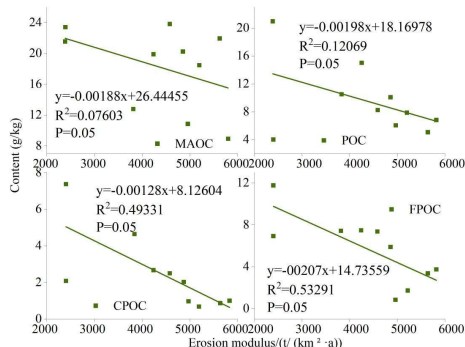


Figure 4: Regression analysis of erosion modules and soil organic carbon content

IV. Conclusion

In this paper, the Kriging interpolation method, random forest algorithm and geographically weighted regression model were comprehensively applied to analyze the distribution of organic carbon in erosion gullies in Heilongjiang Province. The MAOC levels of erosion gullies in agricultural fields, grassy beaches, mudflats, and shallow water areas in eight sampling points were the highest at $14.66\pm 1.15\text{g/kg}$, $25.25\pm 4.64\text{g/kg}$, $25.41\pm 4.56\text{g/kg}$, $64.54\pm 1.61\text{g/kg}$, $25.41\pm 4.56\text{g/kg}$, and $64.54\pm 1.61\text{g/kg}$, respectively. 1.61g/kg , with significant differences ($P < 0.05$) among the sampling sites. The distribution of vertical content of MAOC in grassy beaches ranged from $9.63\text{--}29.89\text{g/kg}$, and that of mudflats ranged from $11.92\text{--}29.97\text{g/kg}$. The distribution of the vertical content of POC ranged from $1.60\text{--}14.78\text{g/kg}$ for grassy beaches and from $2.43\text{--}18.13\text{g/kg}$ for mudflats. The content of the main components of organic carbon decreased with the depth of the soil layer, mainly distributed in $0\text{--}25\text{cm}$. In the regression analysis, the point dispersion of the content of the different components of organic carbon and the number of erosion was small, and the hydraulic erosion affected the organic carbon content of the soil. In the future, the range of sampling points can be expanded, and more erosion gully data can be combined to study the spatial distribution of soil organic carbon and improve the generalization performance of the model.

Funding

This work was supported by:

- National Land Change Survey National Field Verification (Harbin Center) (project number: DD20230517);
- China Geological Survey "Natural Resources Monitoring (Harbin Center)" (project number: DD20243006);
- China Geological Survey Northeast Geological Science and Technology Innovation Center Area Creation Fund project (Study on soil erosion and carbon and nitrogen component migration in sloping cultivated land in southeast Heilongjiang Province) (project number: QCJJ2023-33).

References

- [1] Zhao, Y., Jiang, Q., & Wang, Z. (2019). The system evaluation of grain production efficiency and analysis of driving factors in Heilongjiang province. *Water*, 11(5), 1073.
- [2] Zhang, D., Wang, H., & Lou, S. (2021). Research on grain production efficiency in China's main grain-producing areas from the perspective of grain subsidy. *Environmental Technology & Innovation*, 22, 101530.
- [3] Wang, Z., Zhang, E., & Chen, G. (2023). Spatiotemporal Variation and Influencing Factors of Grain Yield in Major Grain-Producing Counties: A Comparative Study of Two Provinces from China. *Land*, 12(9), 1810.
- [4] Streeter, M. T., & Schilling, K. E. (2020). Assessing and mitigating the effects of agricultural soil erosion on roadside ditches. *Journal of soils and sediments*, 20(1), 524-534.
- [5] Stenberg, L., Tuukkanen, T., Finér, L., Marttila, H., Piirainen, S., Kløve, B., & Koivusalo, H. (2015). Ditch erosion processes and sediment transport in a drained peatland forest. *Ecological Engineering*, 75, 421-433.
- [6] Xu, J., Li, H., Liu, X., Hu, W., Yang, Q., Hao, Y., ... & Zhang, X. (2019). Gully erosion induced by snowmelt in Northeast China: A case study. *Sustainability*, 11(7), 2088.
- [7] Liu, X., Li, H., Zhang, S., Cruse, R. M., & Zhang, X. (2019). Gully erosion control practices in Northeast China: A review. *Sustainability*, 11(18), 5065.
- [8] Wen, Y., Kasielke, T., Li, H., Zepp, H., & Zhang, B. (2021). A case - study on history and rates of gully erosion in Northeast China. *Land Degradation & Development*, 32(15), 4254-4266.
- [9] Zhang, T., Liu, G., Duan, X., & Wilson, G. V. (2016). Spatial distribution and morphologic characteristics of gullies in the Black Soil Region of Northeast China: Hebei watershed. *Physical Geography*, 37(3-4), 228-250.
- [10] Yang, J., Zhang, S., Chang, L., Li, F., Li, T., & Gao, Y. (2017). Gully erosion regionalization of black soil area in northeastern China. *Chinese Geographical Science*, 27, 78-87.
- [11] Liu, L., He, Y., Luo, Z., Gan, Y., You, S., Liu, K., & Du, L. (2024, July). Intelligent Extraction of Erosion Gully from Satellite Images in Northeast China. In *IGARSS 2024-2024 IEEE International Geoscience and Remote Sensing Symposium* (pp. 4128-4131). IEEE.
- [12] Li, M., Li, T., Zhu, L., Meadows, M. E., Zhu, W., & Zhang, S. (2021). Effect of land use change on gully erosion density in the black soil region of Northeast China from 1965 to 2015: a case study of the Kedong County. *Frontiers in Environmental Science*, 9, 652933.
- [13] Tang, J., Xie, Y., Cheng, H., & Liu, G. (2025). Impact of farmland landscape characteristics on gully erosion in the black soil region of Northeast China. *Catena*, 249, 108623.
- [14] Zhao, B., Li, Z., Li, P., Xu, G., Gao, H., Cheng, Y., ... & Feng, Z. (2017). Spatial distribution of soil organic carbon and its influencing factors under the condition of ecological construction in a hilly-gully watershed of the Loess Plateau, China. *Geoderma*, 296, 10-17.
- [15] Cui, L., Li, X., Lin, J., Guo, G., Zhang, X., & Zeng, G. (2022). The mineralization and sequestration of soil organic carbon in relation to gully erosion. *Catena*, 214, 106218.
- [16] O'Rourke, S. M., Angers, D. A., Holden, N. M., & McBratney, A. B. (2015). Soil organic carbon across scales. *Global change biology*, 21(10), 3561-3574.
- [17] Li, Z., Liu, C., Dong, Y., Chang, X., Nie, X., Liu, L., ... & Zeng, G. (2017). Response of soil organic carbon and nitrogen stocks to soil erosion and land use types in the Loess hilly-gully region of China. *Soil and Tillage Research*, 166, 1-9.
- [18] Chaplot, V., & Poesen, J. (2012). Sediment, soil organic carbon and runoff delivery at various spatial scales. *Catena*, 88(1), 46-56.
- [19] Hancock, G. R., Kunkel, V., Wells, T., & Martinez, C. (2019). Soil organic carbon and soil erosion—understanding change at the large catchment scale. *Geoderma*, 343, 60-71.
- [20] Tian, J., Yuan, Y., Zhou, P., Wang, L., Chen, Z., & Chen, Q. (2023). Spatial distribution of soil organic carbon and total nitrogen in a micro-catchment of northeast China and their influencing factors. *Sustainability*, 15(8), 6355.